Supplemental Inventory:

- Supplemental Experimental Procedures

- Supplemental Figure Titles and Legends
  - Figure S1: Phenotypes of *miR-263a* mutant midgut. Related to Figure 1.
  - Figure S2: Quantitative analyses of JAK/STAT and EGFR pathway ligands. Related to Figure 2.
  - Figure S3: *miR-263a* regulates the expression of *Nach* to maintain ISC homeostasis. Related to Figure 3.
  - Figure S4: Increased intracellular Na^+ amount in the midgut epithelium in *miR-263a* mutant. Related to Figure 4.
  - Figure S5: Increased transcript levels of *dcy* and *Hml* in *miR-263a* mutant midguts. Related to Figure 5.
  - Figure S6: *miR-263a* Mutants Disrupt Intestinal pH Homeostasis. Related to Figure 6.
  - Figure S7: Proposed therapeutic potential of *miR-183* for targeting ENaC activity in CF. Related to Figure 7.
  - Table S1: Related to Figure 3.

- Supplemental References

Figure S1

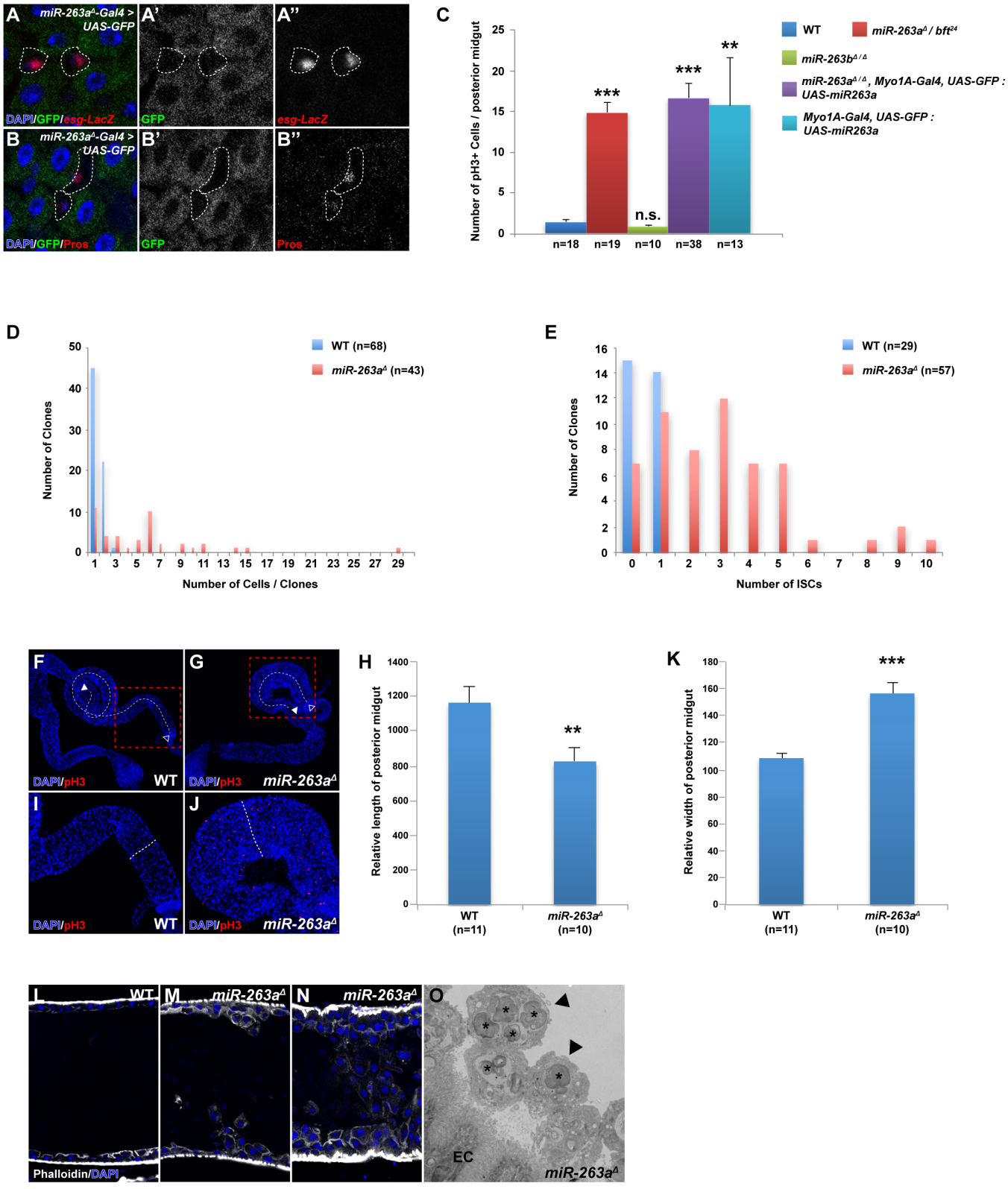
A
miR-263aΔ-Gal4 > UAS-GFP
A'
A''
DAPI/GFP/esg-LacZ
GFP
esg-LacZ
B
miR-263aΔ-Gal4 > UAS-GFP
B'
B''
DAPI/GFP/Pros
GFP
Pros
C
Number of pH3+ Cells / posterior midgut
WT
miR-263aΔ / bft24
miR-263bΔ/Δ
miR-263aΔ/Δ, Myo1A-Gal4, UAS-GFP : UAS-miR263a
Myo1A-Gal4, UAS-GFP : UAS-miR263a
***
***
**
n.s.
n=18
n=19
n=10
n=38
n=13
D
WT (n=68)
miR-263aΔ (n=43)
Number of Clones
Number of Cells / Clones
E
WT (n=29)
miR-263aΔ (n=57)
Number of Clones
Number of ISCs
F
DAPI/pH3
WT
G
DAPI/pH3
miR-263aΔ
I
DAPI/pH3
WT
J
DAPI/pH3
miR-263aΔ
H
Relative length of posterior midgut
**
WT (n=11)
miR-263aΔ (n=10)
K
Relative width of posterior midgut
***
WT (n=11)
miR-263aΔ (n=10)
L
WT
Phalloidin/DAPI
M
miR-263aΔ
N
miR-263aΔ
O
EC
miR-263aΔ

Figure S2

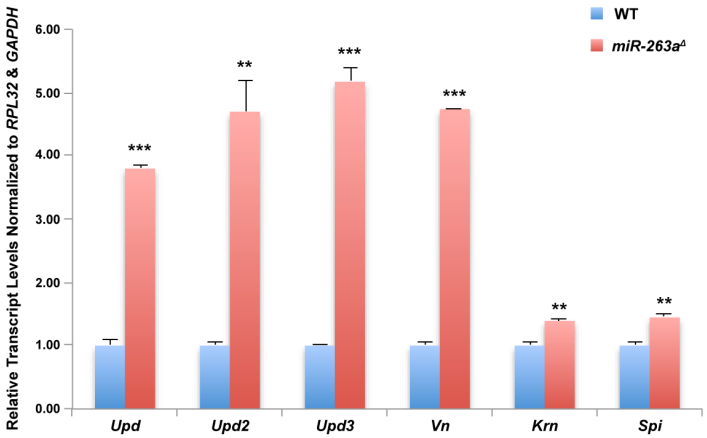
WT
miR-263a^Δ
Relative Transcript Levels Normalized to RPL32 & GAPDH
6.00
5.00
4.00
3.00
2.00
1.00
0.00
***
**
***
***
**
**
Upd
Upd2
Upd3
Vn
Krn
Spi

Figure S3

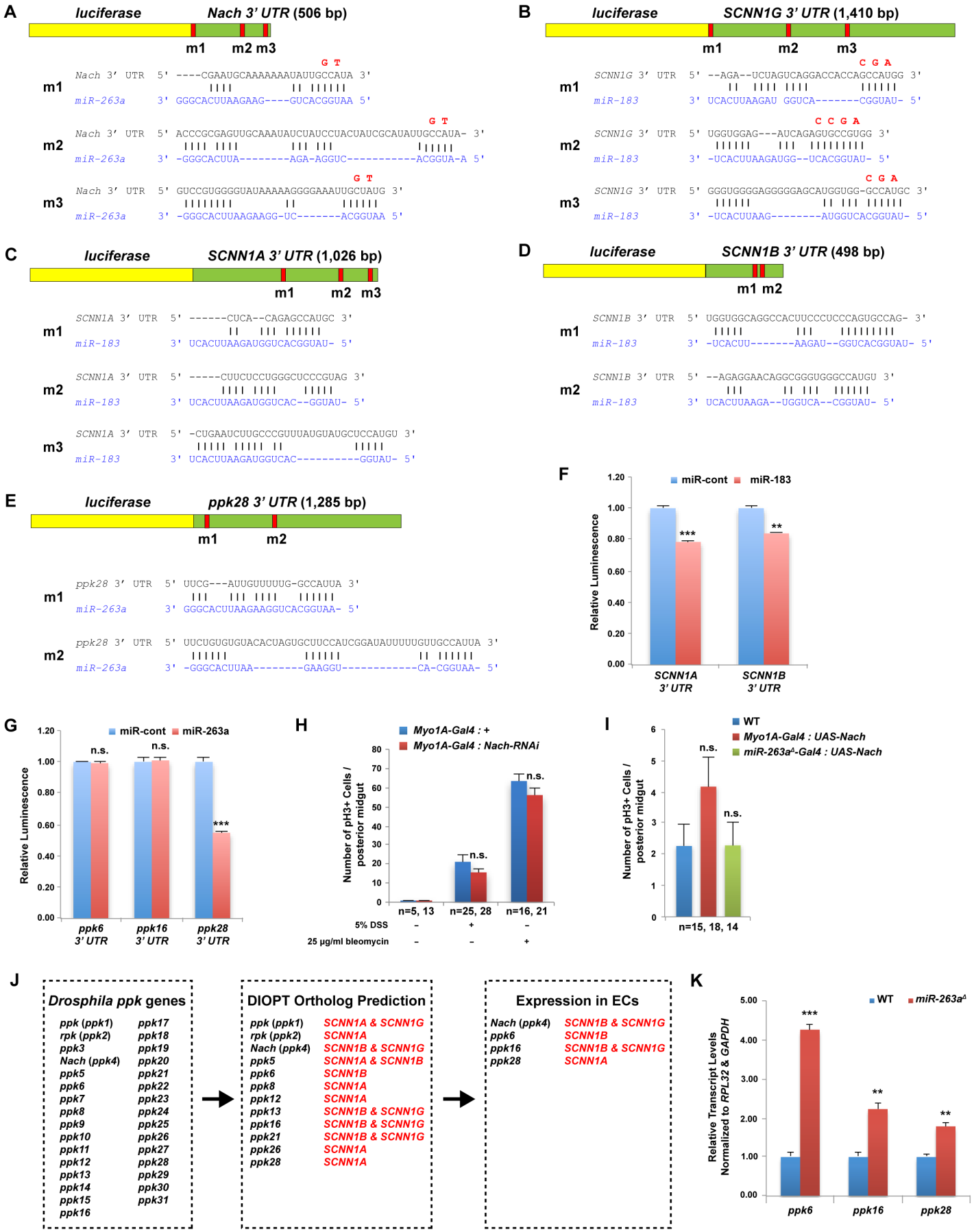
A
luciferase
Nach 3′ UTR (506 bp)
m1
m2 m3
m1
Nach 3′ UTR 5′ ----CGAAUGCAAAAAAAUAUUGCCAUA 3′
miR-263a 3′ GGGCACUUAAGAAG----GUCACGGUAA 5′
m2
Nach 3′ UTR 5′ ACCCGCGAGUUGCAAAUAUCUAUCCUACUAUCGCAUAUUGCCAUA- 3′
miR-263a 3′ -GGGCACUUA--------AGA-AGGUC----------ACGGUA-A 5′
m3
Nach 3′ UTR 5′ GUCCGUGGGGUAUAAAAAGGGGAAAUUGCUAUG 3′
miR-263a 3′ -GGGCACUUAAGAAGG-UC-------ACGGUAA 5′
B
luciferase
SCNN1G 3′ UTR (1,410 bp)
m1
m2
m3
m1
SCNN1G 3′ UTR 5′ --AGA--UCUAGUCAGGACCACCAGCCAUGG 3′
miR-183 3′ UCACUUAAGAU GGUCA-------CGGUAU- 5′
m2
SCNN1G 3′ UTR 5′ UGGUGGAG---AUCAGAGUGCCGUGG 3′
miR-183 3′ -UCACUUAAGAUGG--UCACGGUAU- 5′
m3
SCNN1G 3′ UTR 5′ GGGUGGGGAGGGGGAGCAUGGUGG-GCCAUGC 3′
miR-183 3′ -UCACUUAAG--------AUGGUCACGGUAU- 5′
C
luciferase
SCNN1A 3′ UTR (1,026 bp)
m1
m2
m3
m1
SCNN1A 3′ UTR 5′ ------CUCA--CAGAGCCAUGC 3′
miR-183 3′ UCACUUAAGAUGGUCACGGUAU- 5′
m2
SCNN1A 3′ UTR 5′ -----CUUCUCCUGGGCUCCCGUAG 3′
miR-183 3′ UCACUUAAGAUGGUCAC--GGUAU- 5′
m3
SCNN1A 3′ UTR 5′ -CUGAAUCUUGCCCGUUUAUGUAUGCUCCAUGU 3′
miR-183 3′ UCACUUAAGAUGGUCAC----------GGUAU- 5′
D
luciferase
SCNN1B 3′ UTR (498 bp)
m1
m2
m1
SCNN1B 3′ UTR 5′ UGGUGGCAGGCCACUUCCCUCCCAGUGCCAG- 3′
miR-183 3′ -UCACUU-------AAGAU--GGUCACGGUAU- 5′
m2
SCNN1B 3′ UTR 5′ --AGAGGAACAGGCGGGUGGGCCAUGU 3′
miR-183 3′ UCACUUAAGA--UGGUCA--CGGUAU- 5′
E
luciferase
ppk28 3′ UTR (1,285 bp)
m1
m2
m1
ppk28 3′ UTR 5′ UUCG---AUUGUUUUUG-GCCAUUA 3′
miR-263a 3′ GGGCACUUAAGAAGGUCACGGUAA- 5′
m2
ppk28 3′ UTR 5′ UUCUGUGUGUACACUAGUGCUUCCAUCGGAUAUUUUUGUUGCCAUUA 3′
miR-263a 3′ -GGGCACUUAA--------GAAGGU-----------CA-CGGUAA- 5′
F
miR-cont
miR-183
Relative Luminescence
1.20
1.00
0.80
0.60
0.40
0.20
0.00
***
**
SCNN1A 3′ UTR
SCNN1B 3′ UTR
G
miR-cont
miR-263a
Relative Luminescence
1.20
1.00
0.80
0.60
0.40
0.20
0.00
n.s.
n.s.
***
ppk6 3′ UTR
ppk16 3′ UTR
ppk28 3′ UTR
H
Myo1A-Gal4 : +
Myo1A-Gal4 : Nach-RNAi
Number of pH3+ Cells / posterior midgut
80
70
60
50
40
30
20
10
0
n.s.
n.s.
n.s.
n=5, 13
n=25, 28
n=16, 21
5% DSS
25 µg/ml bleomycin
I
WT
Myo1A-Gal4 : UAS-Nach
miR-263aΔ-Gal4 : UAS-Nach
Number of pH3+ Cells / posterior midgut
6
5
4
3
2
1
0
n.s.
n.s.
n=15, 18, 14
J
Drosphila ppk genes
ppk (ppk1)
rpk (ppk2)
ppk3
Nach (ppk4)
ppk5
ppk6
ppk7
ppk8
ppk9
ppk10
ppk11
ppk12
ppk13
ppk14
ppk15
ppk16
ppk17
ppk18
ppk19
ppk20
ppk21
ppk22
ppk23
ppk24
ppk25
ppk26
ppk27
ppk28
ppk29
ppk30
ppk31
DIOPT Ortholog Prediction
ppk (ppk1) SCNN1A & SCNN1G
rpk (ppk2) SCNN1A
Nach (ppk4) SCNN1B & SCNN1G
ppk5 SCNN1A & SCNN1B
ppk6 SCNN1B
ppk8 SCNN1A
ppk12 SCNN1A
ppk13 SCNN1B & SCNN1G
ppk16 SCNN1B & SCNN1G
ppk21 SCNN1B & SCNN1G
ppk26 SCNN1A
ppk28 SCNN1A
Expression in ECs
Nach (ppk4) SCNN1B & SCNN1G
ppk6 SCNN1B
ppk16 SCNN1B & SCNN1G
ppk28 SCNN1A
K
WT
miR-263aΔ
Relative Transcript Levels Normalized to RPL32 & GAPDH
5.00
4.00
3.00
2.00
1.00
0.00
***
**
**
ppk6
ppk16
ppk28

Figure S4

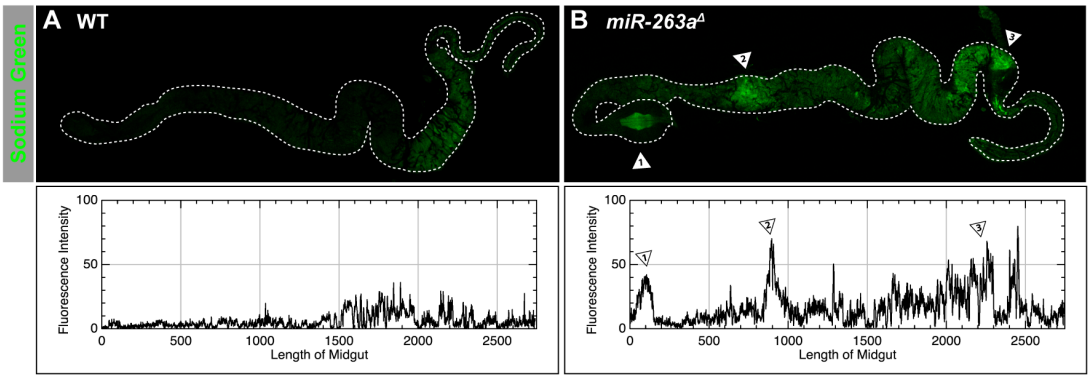
A WT
B miR-263a^Δ
Sodium Green
Fluorescence Intensity
Length of Midgut
100
50
0
0
500
1000
1500
2000
2500
1
2
3

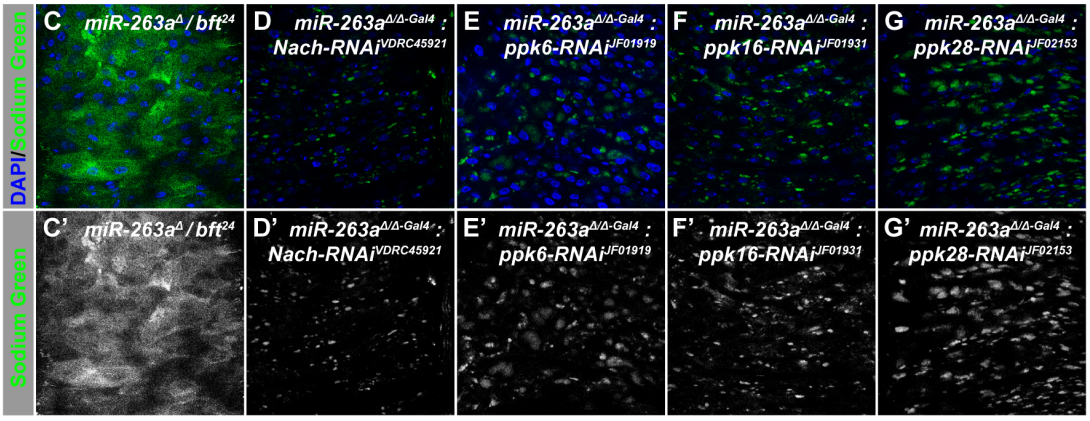
C miR-263a^Δ / bft^24
D miR-263a^Δ/Δ-Gal4 : Nach-RNAi^VDRC45921
E miR-263a^Δ/Δ-Gal4 : ppk6-RNAi^JF01919
F miR-263a^Δ/Δ-Gal4 : ppk16-RNAi^JF01931
G miR-263a^Δ/Δ-Gal4 : ppk28-RNAi^JF02153
DAPI/Sodium Green
C' miR-263a^Δ / bft^24
D' miR-263a^Δ/Δ-Gal4 : Nach-RNAi^VDRC45921
E' miR-263a^Δ/Δ-Gal4 : ppk6-RNAi^JF01919
F' miR-263a^Δ/Δ-Gal4 : ppk16-RNAi^JF01931
G' miR-263a^Δ/Δ-Gal4 : ppk28-RNAi^JF02153
Sodium Green

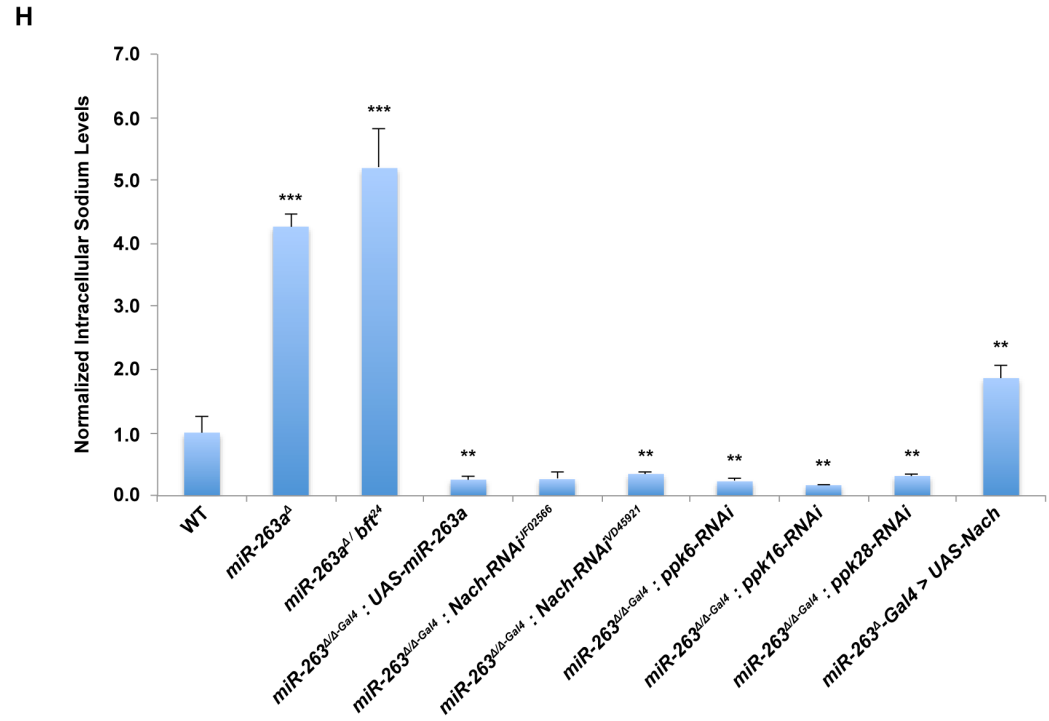
H
Normalized Intracellular Sodium Levels
7.0
6.0
5.0
4.0
3.0
2.0
1.0
0.0
***
***
**
**
**
**
**
**
WT
miR-263a^Δ
miR-263a^Δ / bft^24
miR-263^Δ/Δ-Gal4 : UAS-miR-263a
miR-263^Δ/Δ-Gal4 : Nach-RNAi^JF02566
miR-263^Δ/Δ-Gal4 : Nach-RNAi^JF04521
miR-263^Δ/Δ-Gal4 : ppk6-RNAi
miR-263^Δ/Δ-Gal4 : ppk16-RNAi
miR-263^Δ/Δ-Gal4 : ppk28-RNAi
miR-263^Δ-Gal4 > UAS-Nach

Figure S5

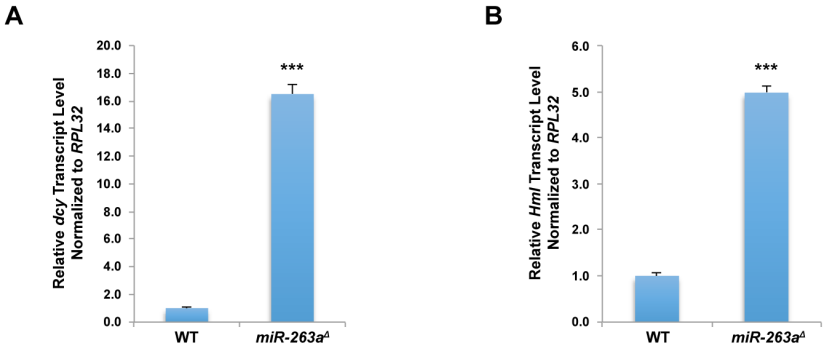
A
Relative dcy Transcript Level
Normalized to RPL32
20.0
18.0
16.0
14.0
12.0
10.0
8.0
6.0
4.0
2.0
0.0
***
WT
miR-263aΔ
B
Relative Hml Transcript Level
Normalized to RPL32
6.0
5.0
4.0
3.0
2.0
1.0
0.0
***
WT
miR-263aΔ

Figure S6

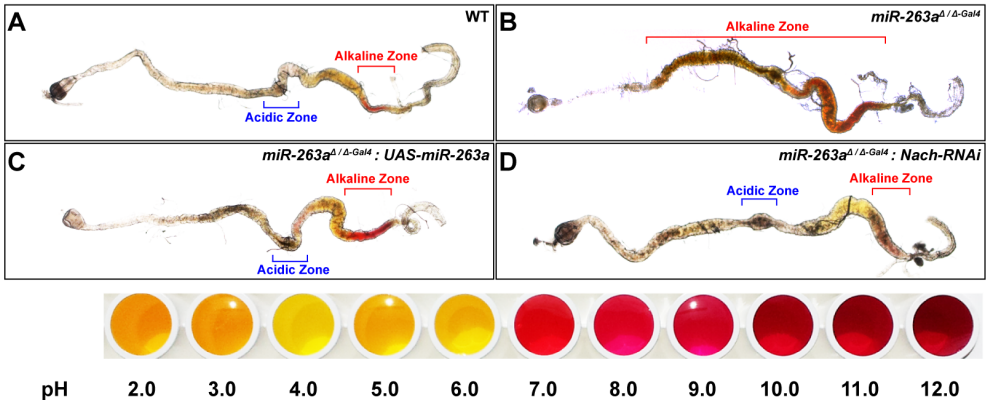
A
WT
Alkaline Zone
Acidic Zone
B
miR-263aΔ / Δ-Gal4
Alkaline Zone
C
miR-263aΔ / Δ-Gal4 : UAS-miR-263a
Alkaline Zone
Acidic Zone
D
miR-263aΔ / Δ-Gal4 : Nach-RNAi
Acidic Zone
Alkaline Zone
pH
2.0
3.0
4.0
5.0
6.0
7.0
8.0
9.0
10.0
11.0
12.0

Figure S7

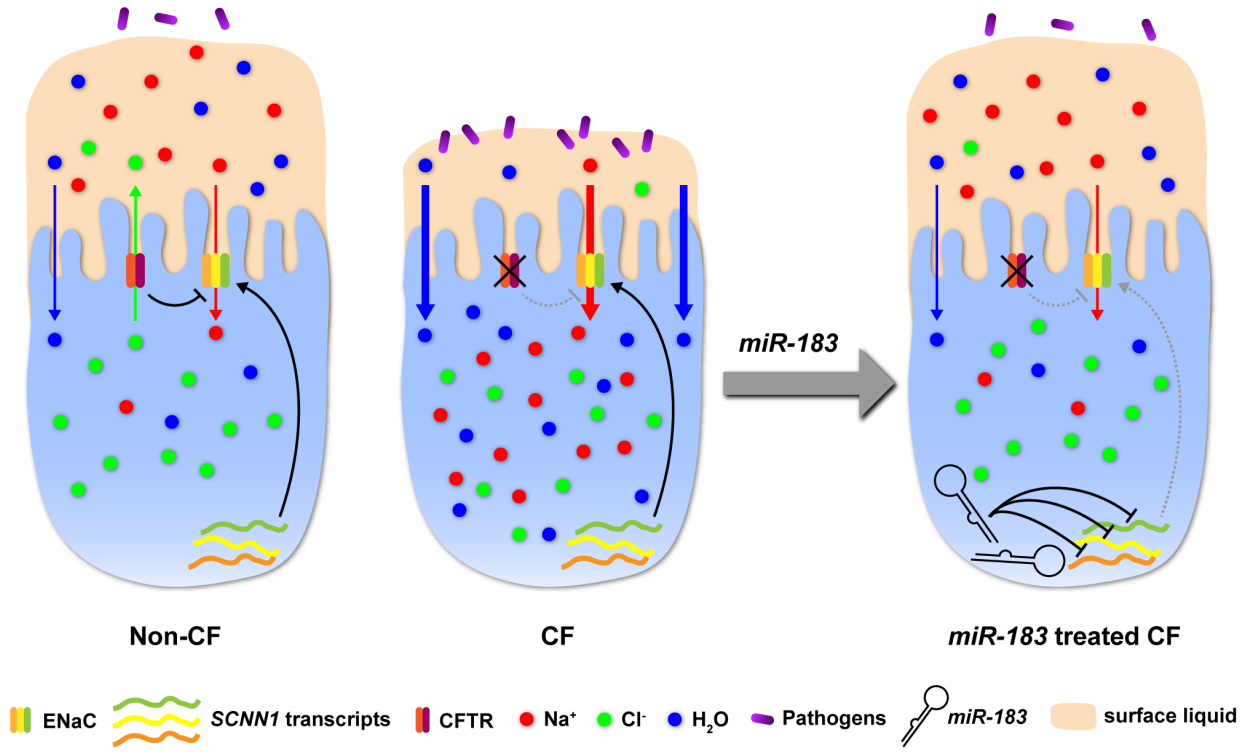
miR-183
Non-CF
CF
miR-183 treated CF
ENaC
SCNN1 transcripts
CFTR
Na+
Cl-
H2O
Pathogens
miR-183
surface liquid

Table S1

Genes	Average Transcript Levels Normalized to RPL32 & GAPDH (*miR-263a*$^{\Delta}$ / wild-type)	Standard Deviation (±)
Nach	41.01	8.16
CG9864	3.76	0.91
PGRP-LF	2.16	0.63
Sras	2.13	0.25
CG7888	2.05	0.62
CG10182	1.96	0.48
Ras85D	1.87	0.12
fkh	1.86	0.18
CG34236	1.71	0.21
dap	1.69	1.09
CG9636	1.58	0.34
CG14131	1.58	0.53
CG6074	1.56	0.83
CG5835	1.43	0.51
Vap-33-1	1.29	0.03
Tango11	1.27	0.20
Sema-5c	1.26	0.20
fz4	1.20	0.13
Gp150	1.18	0.17
mew	1.13	0.13
Calx	1.12	0.18
Lnk	1.12	0.07
Myo31DF	1.09	0.29
NFAT	1.05	0.16
Nak	1.03	0.15
CG8483	0.97	0.22
CG10512	0.93	0.16
Gyc76C	0.89	0.05
CG9238	0.80	0.14
net	0.70	0.15
CG5130	0.67	0.26
Wrinkled	0.63	0.15

Supplemental Experimental Procedures

qPCR. Total RNA was prepared from dissected adult posterior midguts and RNA was extracted using TRIzol Reagent (Invitrogen). cDNA was prepared using NCode EXPRESS SYBR GreenER miRNA qRT-PCR Kit (Invitrogen) and qPCR was performed using iQ SYBR Green Supermix (Bio-Rad). Both *RPL32* and *GAPDH* were used to normalize the RNA levels. cDNAs from CFBE41o- cells were prepared using SuperScript II (Invitrogen). Gene specific primers were used to amplify individual ENaC subunits. qPCR was performed using iQ SYBR Green Supermix (Bio-Rad) and human *GAPDH* was used to normalize the RNA levels. Relative quantification of mRNA levels was calculated using the comparative CT method. Following primer sequences were used:

Gene specific primers for RT
SCNN1A: 5'-CATCAACCTCAACTCGGACA-3'
SCNN1B: 5'-CCCTCACAGATGATGCGCTT-3'
SCNN1G: 5'-GCAGGATGAGTATCCCTTCG-3'
human *GAPDH*: 5'-GGCTGTTGTCATACTTCTCATGG-3'

qPCR primers
Nach F: 5'-TTCAACATGCAAAAGTCCGAGG-3'
Nach R: 5'-ACAGCGATACAGAATTTCGTCAC-3'
ppk6 F: 5'-CCCATTCTAAACACCATCTCCAA-3'
ppk6 R: 5'-CGAGTTGACCACCTTCGGA-3'
ppk16 F: 5'-AGGACATCAGTCGCCATGAG-3'
ppk16 R: 5'-GCTCCAGTACCAGGACACC-3'
ppk28 F: 5'-GCCGAAGAGAGCATCACCATT-3'
ppk28 R: 5'-AGAACACGGAAAGGATCACCA-3'
RPL32 F: 5'-AGCATACAGGCCCAAGATCG-3'
RPL32 R: 5'-TGTTGTCGATACCCTTGGGC-3'
GAPDH F: 5'-CATTGTGGGCTCCGGCAA-3'
GAPDH R: 5'-CGCCCACGATTTTCGCTATG-3'
SCNN1A F: 5'-CTTTGGCATGATGTACTGGCA-3'
SCNN1A R: 5'-GGAAGACGAGCTTGTCCGAGT-3'
SCNN1B F: 5'-GCCCTTCAGCAGGTACTTCTT-3'
SCNN1B R: 5'-GTGTCCCAGTGTCACCAACA-3'
SCNN1G F: 5'-GCACCCGGAGAGAAGATCAAA-3'
SCNN1G R: 5'-TACCACCGCATCAGCTCTTTA-3'
human *GAPDH* F: 5'-AATCCCATCACCATCTTCCA-3'
human *GAPDH* R: 5'-TGGACTCCACGACGTACTCA-3'
Upd F: 5'-CAGCGCACGTGAAATAGCAT-3'
Upd R: 5'-CGAGTCCTGAGGTAAGGGGA-3'
Upd2 F: 5'-TTCTCCGGCAAATCAGAGATCC-3'
Upd2 R: 5'-GCGCTTGATAACTCGTCCTTG-3'
Upd3 F: 5'-AGCCGGAGCGGTAACAAAA-3'
Upd3 R: 5'-CGAGTAAGATCAGTGACCAGTTC-3'
Vn F: 5'-GAACGCAGAGGTCACGAAGA-3'
Vn R: 5'-GAGCGCACTATTAGCTCGGA-3'
Krn F: 5'-CCGCTTTAATCGGCGCTTAC-3'
Krn R: 5'-ATCGGGAAGGTGACATTCGG-3'
Spi F: 5'-TGCGGTGAAGATAGCCGATC-3'
Spi R: 5'-TTCGCATCGCTGTCCCATAA-3'
AttA F: 5'-CACAACTGGCGGAACTTTGG-3'
AttA R: 5'-AAACATCCTTCACTCCGGGC-3'
Dpt F: 5'-CGTCGCCTTACTTTGCTGC-3'
Dpt R: 5'-CCCTGAAGATTGAGTGGGTACTG-3'
Rel F: 5'-GGTGATAGTGCCCTGCATGT-3'
Rel R: 5'-CCATACCCAGCAAAGGTCGT-3'
dcy F: 5'-ATGAAACGGACATACTTGTTGCT-3'

dcy R: 5'-CTGCTGAAGGTTGGAGGACTT-3'
Hml F: 5'-GGAGAACGAACGGAACGAAC-3'
Hml R: 5'-CTACGGCCTCCTTCAGAACC-3'

Luciferase reporter assays. Luciferase reporter plasmids containing 3' UTRs of *Nach*, *ppk6*, *ppk16*, *ppk28*, *SCNN1A*, *SCNN1B*, and *SCNN1G* were constructed using the following primers as previously described (Kim et al., 2014):

Nach F: 5'-CTAGCTAGCTCAGCACGATGGGCGAATGCAAA-3'
Nach R: 5'-CCGAGCTCGACGATGGTGTTGCGATTG-3'
ppk6 F: 5'-CGGAATTCAGCAAATACAAAAAAAAAGAAATTATGGTATCT-3'
ppk6 R: 5'-CGGGATCCATCGATGATTTCCTACCCCCCGCACA-3'
ppk16 F: 5'-CGGAATTCAGTGGCAGTTCCCAGCCATCTTC-3'
ppk16 R: 5'-CGGGATCCTGTGTTTGAAGAGTGCACGAGTTC-3'
ppk28 F: 5'-CCCTCGAGATAAATATATCGAAATATACCAAAATATATGC-3'
ppk28 R: 5'-CCGAGCTCTCACTGACTAAGCCCATAAACA-3'
SCNN1A F: 5'-CGGAATTCGAGGGAAGGAGAGGTTTCTCACACCA-3'
SCNN1A R: 5'-CGGGATCCTTCATGCAACAAACATTTATTGAGCTC-3'
SCNN1B F: 5'-CGGAATTCCCCTGCCCCTGCCCACCCCGGGC-3'
SCNN1B R: 5'-CGGGATCCTGGACTCAGTATTTTCTACTTTTATTTTCTA-3'
SCNN1G F: 5'-CTAGCTAGCGGCAGGGTTGAGAAGACAGATCTAG-3'
SCNN1G R: 5'-CCGAGCTCTTTAGGGTTTGCTGGCTTTG-3'

The human *miR-183* overexpression plasmid was constructed by amplifying 399 nt fragment from HEK293 genomic DNA using specific primers (F, 5'-GGGGTACCAAGGTCATCTTGGGCTGATG-3'; R, 5'-GCTCTAGATCTCTGGGGACACACTGGAC-3'). Amplified fragment was digested with *KpnI* and *XbaI*, and was ligated into the linearized *pAc5.1/V5-His C* vector. To mutate the seed sequences of *miR-263a* and *miR-183* binding sites within the 3' UTRs of *Nach* and *SCNN1G*, we followed the instructions of QuikChange II XL Site-Directed Mutagenesis Kit (Stratagene). *Drosophila* S2R+ cells were maintained in Schneider's *Drosophila* Medium (Gibco) with 10% heat-inactivated FBS (Sigma) and 1% Pen/Strep (Gibco) at 25°C. Experiments were performed in 96-well plates excluding the outer wells. Cells were transfected with 40 ng of plasmid expressing *pAc-miRNAs*, 10 ng of firefly luciferase reporter plasmid and 10 ng of *Renilla* luciferase reporter plasmid for transfection control, using Effectene Transfection Reagent (Qiagen). After 72 h, luciferase activities were measured using DualGlo (Promega).

Supplemental Figure Titles and Legends

Figure S1. Phenotypes of *miR-263a* mutant midgut. Related to Figure 1. (A-B'') *miR-263a$^{\Delta}$-Gal4* expression in the posterior midgut was visualized by the expression of GFP. **(A-A'')** GFP expression is absent in ISCs and EBs, which are marked by nuclear *esg-LacZ* (green) and white dotted lines outline the ISCs and EBs lacking LacZ expression. **(B-B'')** GFP expression is also absent in EEs as visualized by the lack of GFP signal in cells expressing Pros (red), a nuclear marker of EE. White dotted lines outline the EEs lacking LacZ expression. **(C)** The average number of pH3+ cells in the posterior midgut at 14 days old. Like *miR-263a$^{\Delta}$* homozygous mutants, *miR-263a$^{\Delta}$* and *bft^{24}*, a previously characterized mutant allele of *miR-263a*, trans-heterozygotes increase the number of pH3+ cells. Homozygous null mutants of *miR-263b* (*miR-263b$^{\Delta}$*) did not perturb ISC homeostasis. Unlike overexpression of *UAS-miR-263a* using *miR-263a$^{\Delta}$-Gal4* (**Figure 1E**), overexpression of *miR-263a* using an EC specific *Myo1A-Gal4* in the *miR-263a* mutant background did not suppress the increase in pH3+ cells. This is likely due to different strengths of the *Gal4* drivers used. Since *Myo1A-Gal4*, compared to the *miR-263a$^{\Delta}$-Gal4*, is a much stronger *Gal4* driver, overexpressing *miR-263a* beyond its normal physiological levels might now target non-physiological targets of *miR-263a*, which may also affect ISC homeostasis. In support of this hypothesis, overexpression of *miR-263a* using *Myo1A-Gal4* in a wild-type background significantly increased the number of pH3+ cells. "n" denotes the number of posterior midguts examined for each genotype. **(D)** Quantification of cell number in each clone. *miR-263a* mutant clones frequently contain more cells. **(E)** Quantification of ISCs in each clone. *miR-263a* mutant clones frequently contain more ISCs. "n" denotes the number of clones examined for each genotype. **(F-G)** The whole adult midgut of wild-type and *miR-263a* mutant stained with anti-pH3 (red) and DAPI (blue). Dotted lines were measured to quantify the posterior midgut lengths (hindgut [open arrowhead] to copper cell region [solid arrowhead]). **(H)** The average relative length of posterior midguts of wild-type and *miR-263a* mutants. **(I-J)** Magnified view of the posterior midgut region from **(F-G)**, red dotted box. The dotted lines were measured to quantify posterior midgut width. **(K)** The average relative width of posterior midguts of wild-type and *miR-263a* mutants. "n" denotes the number of posterior midguts examined for each genotype. **(L-N)** Cross-section view of the wild-type **(L)** and *miR-263a* mutants **(M-N)** posterior midgut stained with phalloidin (green) and DAPI (blue). The wild-type epithelium is normally a monolayer of ECs **(L)**, but *miR-263a* mutants frequently show mild **(M)** to severe **(N)** multi-layering of ECs. **(O)** EM section of the *miR-263a* mutant posterior midgut. ECs undergoing delamination and anoikis (arrowheads) as evident by the presence of large lysosomes (asterisks) was frequently observed in *miR-263a* mutants. Error bars indicate SEM. **P < 0.05 and ***P < 0.001 (two-tailed t-test).

Figure S2. Quantitative analyses of JAK/STAT and EGFR pathway ligands. Related to Figure 2. The relative mRNA levels of JAK/STAT and EGFR pathway ligands in the posterior midguts were measured by qPCR. Increased expression of all ligands was observed in the *miR-263a* mutant midgut. Error bars indicate SEM. **P < 0.05 and ***P < 0.001 (two-tailed t-test).

Figure S3. *miR-263a* regulates the expression of *Nach* to maintain ISC homeostasis. Related to Figure 3. (A-E) Diagram of the 3' UTR luciferase reporters labeled with potential *miR-263a* and *miR-183* binding sites. Predicted binding sites of *miR-263a* and *miR-183* were mutated as indicated in red to generate a mutated *Nach* and *SCNN1G* 3' UTR reporters **(A-B)**. **(F)** Co-expression of *miR-183* significantly repressed the luciferase activities of wild-type *SCNN1A and SCNN1B* 3' UTR luciferase reporters. **(G)** Co-expression of *miR-263a* significantly repressed the luciferase activity of wild-type *ppk28* 3' UTR luciferase reporters, but not *ppk6* and *ppk16*. **(H)** Depletion of *Nach* by RNAi in a wild-type background did not affect damage induced ISC proliferation by DSS or bleomycin. **(I)** Overexpression of *Nach*, by *miR-263a$^{\Delta}$-Gal4* and *Myo1A-Gal4*, did not increase pH3+ cells. **(J)** There are 31 *ppk* genes in the *Drosophila* genome that represent a family of ion channels called the Degenerin/epithelial sodium channel (DEG/ENaC). Out of 31 *ppk* genes, 12 genes are predicted orthologs of human *SCNN1* genes, of which there are three subunits (*SCNN1A*, *SCNN1B*, and *SCNN1G*). Out of 12 *ppk* genes, 4 genes are expressed in ECs (Doupé and Perrimon, personal communication). **(K)** qPCR analyses of *ppk* genes expressed in ECs using total RNA from dissected posterior midguts of indicated genotypes. Relative transcript levels of all four *ppk* genes are increased in *miR-263a* mutant midguts. Error bars indicate SEM. **P < 0.05 and ***P < 0.001 (two-tailed t-test).

Figure S4. Increased intracellular Na^+ amount in the midgut epithelium in *miR-263a* mutant. Related to Figure 4. (A) Na^+ in the entire length of the control midgut epithelium and **(B)** *miR-263a* mutant. White dotted lines outline the entire length of the midgut. *miR-263a* mutants have increased Na^+ in the anterior and posterior regions of the midgut (white arrowheads). Intensity of Sodium Green flourescene along the entire length of the midgut is plotted below. **(C-C')** Trans-heterozygous mutant of *miR-263a$^{\Delta}$* and *bft^{24}* has significantly higher amount

of intracellular Na^+ as indicated by increased fluorescence. **(D-D')** Depletion of *Nach* using additional independent RNAi line in the *miR-263a* mutant background, also, suppressed the increased Na^+ uptake by the epithelium. **(E-G')** Depleting individual *ppk* genes (*ppk6*, *ppk16* and *ppk28*) in the *miR-263a* mutant background completely suppressed the increased Na^+ uptake by the epithelium. **(H)** Quantifiation of Sodium Green fluorescence. Error bars indicate SEM. **P < 0.05 and ***P < 0.001 (two-tailed t-test).

Figure S5. Increased transcript levels of *dcy* and *Hml* in *miR-263a* mutant midguts. Related to Figure 5. (A) qPCR analysis of *dcy* using total RNA from dissected midguts of indicated genotypes. **(B)** qPCR analysis of *Hml*, a close ortholog of both the human *MUC5AC* and *MUC5B*, using total RNA from dissected midguts of indicated genotypes. Error bars indicate SEM. **P < 0.05 and ***P < 0.001 (two-tailed t-test).

Figure S6. *miR-263a* Mutants Disrupt Intestinal pH Homeostasis. Related to Figure 6. (A-D) Colorimetric monitoring of intestinal pH using phenol red. *miR-263a* mutants disrupt intestinal pH homeostasis by extensive alkalization of midgut **(B)**. Expansion of the alkaline region was significantly suppressed by overexpressing *miR-263a* **(C)** and knocking down *Nach* by RNAi **(D)** in the *miR-263a* mutant background.

Figure S7. Proposed therapeutic potential of *miR-183* for targeting ENaC activity in CF. Related to Figure 7. Under normal conditions, the CFTR pumps Cl^- out of the cells and ENaC absorbs Na^+ into the cells to maintain osmotic homeostasis. In CF, inability to pump Cl^- out of the cells due to loss-of-function mutations in CFTR releases ENaC from its inhibition resulting in hyper-absorption of Na^+ and increased driving force for water reabsorption into the cells. Consequently, increased water reabsorption contributes to chronic dehydration of the protective surface liquid that lines the epithelium. Given our findings that human miRNA, *miR-183*, can directly regulate the expression of all three ENaC subunits, *miR-183* might present itself as a potential therapeutic agent for regulating ENaC activity in CF.

Table S1. Related to Figure 3. Average qPCR quantification (3 replicates) of transcript levels for 32 genes, which are predicted targets of *miR-263a* (TargetScan) and are expressed in ECs. Top five genes had transcript levels of >2-fold on average (blue) in the mutant compared to the control.

Supplemental References

Kim, K., Vinayagam, A., and Perrimon, N. (2014). A rapid genome-wide microRNA screen identifies miR-14 as a modulator of Hedgehog signaling. Cell Rep *7*, 2066-2077.